Characteristics of temperature-dependent shear flow in an ultrasonicated ferrofluid

Ibiyemi A. Abideen*

Department of Physics, Federal University, Oye-Ekiti, Nigeria

ARTICLE INFO

ABSTRACT

The rheological effect of manganese zinc (Mn-Zn) ferrite ferrofluid was studied and the impact of temperature on the magnetoviscosity and viscoelastic system of manganese-zinc ferrite ferrofluid generated by co-precipitation process is investigated. At 25 °C, a ferrofluid structure that is both hard and elastic is produced. As the temperature rises, the fluid structure loses its elasticity and becomes semi-rigid. When a low relaxation modulus is applied, the fluid behavior, which is temperature-dependent, exhibits the development of linear stress relaxation and steady state flow. When a greater relaxation modulus is used, non-steady state flow results. At a high temperature of 50 °C, steady state flow is quickly obtained, whereas at a low temperature, equilibrium or steady state is attained more slowly. At low temperatures, the fluid exhibits a solid-like structure, whereas at high temperatures, a liquid-like structure forms as the fluid's viscosity decreases. With the creation of yield stress in the region with high shear rates, shear stress increases with temperature, and yield stress increases with temperature. The viscoelastic system is underdamped, and the amount of fluid deflected at 25 °C is small, which prevents the disruption of the fluid's rheology. This develops as a result of the presence of a small deflection angle, which facilitates the development of high magnetoviscosity at low temperature. High viscous effect forms at low temperatures due to the creation of low shear stress and low deflection angle at temperature 25 °C. The sample has a single phase and FCC structure, which X-ray diffraction research has verified.

1. INTRODUCTION

Due to its extraordinary magnetic effects, magnetic nanoparticles have recently played significant roles in device application. Some ferrite materials' particles, including ferrite made of zinc, manganese, cobalt, nickel, and other metals, naturally possess extraordinary magnetic characteristics and respond well to magnetic fields. The design of significant devices, such as transducers, heat control devices, dampers, heat exchange, magneto-optical devices, magnetorheological fluid (MR fluid), and ferrofluid, is aided by the magnetic nanoparticles' response to magnetic fields [1–4]. Magnetic particles are helpful in medicine as a drug delivery agent and for treating hyperthermia [5]. This study focuses on the utilization of ferrofluid made of magnetic nanoparticles. Small magnetic particles contained in a non-

*Corresponding author: Tel.: +2348062198624
e-mail: abideen.ibiyemi@fuoye.edu.ng (Ibiyemi A. Abideen)

magnetic medium make up ferrofluid, which also contains a carrier liquid, and nanomagnetic particles as its main components. It is created by scattering nanomagnetic particles in a carrier media like kerosene, paraffin, or water. When exposed to an external magnetic field, it significantly alters its rheological behavior. A complicated system with several conflicting forces, such as magnetostatic force, Van der Walls attractive force, Brownian motion, attractive gravitational force, and steric repulsion, can benefit from ferrofluid. These forces must be balanced in order to generate a stable dispersion, with the repulsive forces dominating the attractive forces to prevent flocculation during the disperse phase.

Prior to the development of ferrofluid, MR fluid, a magnetic fluid composed of micron-sized magnetic particles dispersed in a non-magnetic medium, was used in a variety of technical applications. However, due to its drawbacks, MR fluid later became ineffective and was replaced by ferrofluid. Micron-sized magnetic particles suspended in a non-magnetic liquid make up MR fluid. Complex fluids known as MR fluids undergo rheological changes due to influence of a magnetic field [6]. Shear stress, viscosity, and settling rate are the fluid's most notable properties, which structured it to be appropriate for industrial applications [7]. By optimizing specific variables like temperature, shear rate, and magnetic field, these properties can be balanced [8]. Due to issues with the rheology of the fluid, such as settling rate and particle aggregation, the performance of MR fluid is limited to certain applications [9]. Procedures like the use of surfactants or thixotropic chemicals were adopted to address these issues. According to recent reports from various studies, using ferrofluid is a wonderful method for reducing the pace at which micron-sized particles settle in MR fluid [10]. The micron-sized particles are polarized and organize themselves into chains or clusters through dipole-dipole interaction when a magnetic field is applied across the fluid particles. The clusters also create tiny voids within the nanostructures. Colloidal nanobridges (CNBs) are created by the ferrofluid's nanoscale particles filling up these cavities [11]. The fluid is now more stable and suited for a variety of technical uses, including lubricants, dampers, clutches, and bearings [12]. The effect of thermal energy is one of the primary factors that is used to optimize the rheology of the magnetic nanofluid. Literature indicates that at high temperature, the fluid particle has high thermal energy that the particle aggregate could not withstand. At high thermal application, the chains break down and the particles are dissociated from the aggregate. The application of low temperature leads to the formation of high magnetoviscosity, this occurred because the par.

Ferrofluid is economically helpful in loudspeaker and computer hard drives because it prevents junk, debris, or scraps from entering the computer hard drive, according to the literature. Ferrofluid is used as a heat controller in loudspeakers because it eliminates heat produced by the coils and dampens cone movement. The generated fluid is coated with a surfactant like oleic acid to produce a high-quality ferrofluid. Oleic acid stops particle clumps or bunches from forming in a fluid. Strength of the applied magnetic field and field-induced structure affect ferrofluid characteristics, and its nature is based on how the magnetic particles are distributed hydrodynamically in the base medium. Ferrofluid demonstrated Newtonian behavior at high shear rates
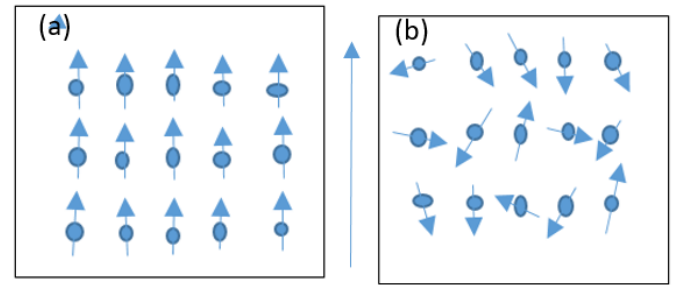

Figure 1. Schematic diagram of particle orientation when (a) magnetic field is applied (b) magnetic field is withdrawn.

when a magnetic field was introduced [13]. The magnetic field's application causes the particles to align in a predictable array and create a structure that resembles a chain. According to Figure 1a, the particles are neatly arranged in the magnetic field's direction. However, when the magnetic field is removed, the particles are placed randomly and out of alignment, as shown in Figure 1b. As a result, the chain aggregate is broken, the field-induced structure is destroyed, and the particle orientation in the liquid medium is random. As a result, the fluid becomes thinner and the magnetoviscosity decreases.

One of the main factors that is used to optimize the rheology of the magnetic nanofluid is the effect of thermal energy. Literature shows that at high temperature, the fluid particle has high thermal energy which the particle aggregate could not withstand. The chains disintegrate and the particles separate from the aggregate at high heat application. Because the particle aggregate can withstand the thermal energy from low temperature, the application of low temperature causes the creation of high magnetoviscosity. As the temperature rises, the viscosity decreases [14], which results from the weakening of the cohesiveness between the interacting particles. As the temperature rises, the average kinetic energy rises as well, forcing the attractive binding energy to vanish [15] and causing the particles to separate from their aggregates. When the particles separate from the aggregates, they become mobile, and as the mobility rises with temperature, the chain holding the particles together is destroyed.

This study's major objective is to conduct an experimental investigation of the effects of temperature and applied shear rates on the rheological characteristics of a co-precipitated, oleic acid-coated Mn-Zn ferrite ferrofluid. The characteristics of the ferrite nanoparticles structure are ascertained using diffraction technique of X-ray, and the surface morphology of the sample is examined using scanning electron microscopy. The oscillatory and rotational mode tests are used to obtain the rheological results. Using a rheometer (MCR 301) at temperatures of 25°C, 40°C, and 50°C, the rheological properties including shear viscosity, complex viscosity, shear stress, loss modulus, storage modulus, relaxation modulus, transmission torque, damping factor, and deflection angle are studied.

2. EXPERIMENTAL DETAILS

The experimental approach for manganese zinc ferrite ferrofluid is schematically depicted in Figure 2. Manganese (II) chloride tetrahydrate ($MnCl_2.4H_2O$), zinc (II) chloride hexahydrate

(ZnCl$_2$.6H$_2$O), and iron (III) chloride (FeCl$_3$) are the three aqueous solutions needed for the manufacture of manganese zinc ferrite magnetic nanoparticles. The reagent beakers were carefully cleaned with distilled water, isopropyl ethanol, and acetone prior to the production of the Mn-Zn ferrite sample. To get rid of any pollutants inside the beakers, they were carefully cleaned [16]. A digitally equipped weighing machine was employed in weighing the necessary quantity of the solutions. We start the synthesis by using a magnetic stirrer to heat the aqueous solutions of ZnCl$_2$.6H$_2$O, MnCl$_2$.4H$_2$O, and FeCl$_3$ at 60 °C for 30 minutes. Magnetic stirring of the solution produces homogeneous solutions. Then, in a single reagent beaker, the solutions of ZnCl$_2$.6H$_2$O, MnCl$_2$.4H$_2$O, and FeCl$_3$ were combined. The reagent beaker is put on the heater and is continually stirred once the solution has been mixed. Drops of ammonia solution are added to the precipitate until the pH level of 11 is reached. Oleic acid was added to the solution. Oleic acid, a surfactant, is included to stop the particle from clumping together. After being decanted, the precipitate is cleaned with distilled water. Acetone was used to purify the precipitates and get rid of any contaminants. After obtaining a wet slurry, the slurry was mixed with kerosene and centrifuged at 12,000 rpm to separate the larger size particles from the medium and create a ferrofluid made of MnZnFe$_2$O$_4$ as a result. Rheological properties were tested using a rheometer at temperatures of 25°C, 40 °C and 50 ° after the nanofluid had formed. The X-ray diffraction patterns of the particles was investigated using Rigaku Ultima multiple X-ray diffractometer. The morphology of the nanoparticles, microstructure, shape, and lattice information were obtained using the Transmission Electron Microscopy (TEM) and High-resolution Transmission Electron Microscopy (HRTEM). Using an MCR-301 rheometer, the sample's viscoelastic characteristics were examined.

3. RESULT AND DISCUSSION

3.1. FOURIER TRANSFORM INFRARED AND ATOMIC WEIGHT COMPOSITION OF THE FERROFLUID

The atom composition of the produced Mn-Zn ferrite magnetic nanoparticles was examined by elemental dispersive X-ray spectroscopy (EDS). The elements and their compositions are shown in Figure 3a, and the histogram displays the weight % of the atoms in various proportions. Zinc, manganese, iron, and oxygen are formed, according to EDS. Since no foreign substances were discovered, the sample is pure Zn$_x$Mn$_{1-x}$Fe$_2$O$_4$ nanomagnetic material. Figure 3b showed the Fourier Transform Infrared (FTIR) spectrometer's absorption bands. The FTIR analysis of the functional groups found in the synthetic material showed that metal oxide, hydroxyl, and carboxylic groups were formed. The development of the C=O stretching vibration, which results in the strong absorption band about 1680 cm^{-1}, shows the presence of the carboxylic group. The production of the hydroxyl group and the O-H bending vibration of the absorbed water are responsible for the weak bands that were discovered about 1380 cm^{-1}. The band that emerged at 1050 cm^{-1} indicates that the nitrate group is beginning to extend vibrationally [17, 18]. Tetrahedral and octahedral metal-oxygen (M-O) bond vibrations are what cause the absorption band to form at a wavelength of 600 cm^{-1}. The creation of the O=C=O stretching vibration of the carboxy-

late group and compound class of carbon dioxide was revealed by the strong absorption band identified approximately at 2400 cm^{-1}. The medium band, which was formed about 2900 cm^{-1}, indicated the presence of the compound class of alkane and the production of C-H stretching in the sample. The bands near 650 cm^{-1} are attributed to the vibration of the C-N=O bending and the presence of the C-C ring. The creation of the faint absorption band at 2700 cm^{-1}, which indicates the existence of the hydroxyl group, can be attributed.

Figure 4 displays the SEM picture of magnetic Mn-Zn ferrite particles. The surface morphology and microstructure of the ferrite sample are examined using SEM. The production of tightly packed structures and the relatively uniform microstructures revealed the formation of particles with spherical shapes and various grain sizes. Particle agglomeration and the presence of a hollow were discovered. The formation of particle aggregation is represented by the ring. Transmission electron microscopy (TEM) and high-resolution transmission electron microscopy (HRTEM) are also used to study the ultrasonicated Mn-Zn ferrite sample. The sample's structure, shape, and particle dispersion were made clear by the TEM. The particles are uniformly dispersed and there is no evidence of particle aggregation. Because the particles were agitated at an ultrasonic frequency prior to TEM analysis, the particle agglomerations visible in the SEM image could not be observed in the TEM image. This exemplifies how sonication affects particle creation. The agitation is carried out ultrasonically at a frequency of 100 Hz. In order to create stable magnetic fluid, the agglomeration must be destroyed. The Mn-Zn ferrite magnetic nanoparticles were visible as multiple aggregated layers piled together with an interlayer spacing of 0.82 nm on the HRTEM. The estimated lattice d-spacing is 0.24 nm. Inset in Figure 5 is the lattice fringe. It provided precise details regarding the atomic structure and lattice spacing. Viewing the grain boundaries and interface from the HRTEM image. It was determined from the TEM image in Figure 5a that the nanofluid is made up of tiny clusters of fundamental particles with sizes between 10 and 15 nm, and the form displayed is spherical. Multiple diffraction peaks without phase transition were visible in the XRD diffraction patterns depicted in Figure 4. The diffraction planes (220), (311), (400), (422), (511), and (440) are corresponding to the peak positions at 2θ = 29.2584, 35.284, 42.827, 52.13, 56.465, and 62.734, respectively. All of the characteristic diffraction peaks of the ferrite spinel crystal are visible in the samples. Unlike NiFe$_2$O$_4$, which shows additional reflections, the sample only shows the FCC structure, excluding the formation of any additional phases [19]. The peaks in the diffraction pattern represent the cubic structure of zinc ferrite (ASTM card no. 22-1086). The multiple peaks imply a polycrystalline nature for the nanoparticles. This result is consistent with the findings of Ibiyemi *et al.*, Mishra *et al.*, and Chand *et al.* [20–22]. Along the reflection plane of (311) is displayed the recommended orientation. Derby Scherer is used to estimate the typical crystallite size, which is 17.46 nm on average, and the samples show a single phase cubic spinel structure.

3.2. SHEAR VISCOSITY AND SHEAR STRESS

The viscosity of Mn-Zn ferrite at various temperatures is depicted in Figure 6a. Recent research demonstrates that the application
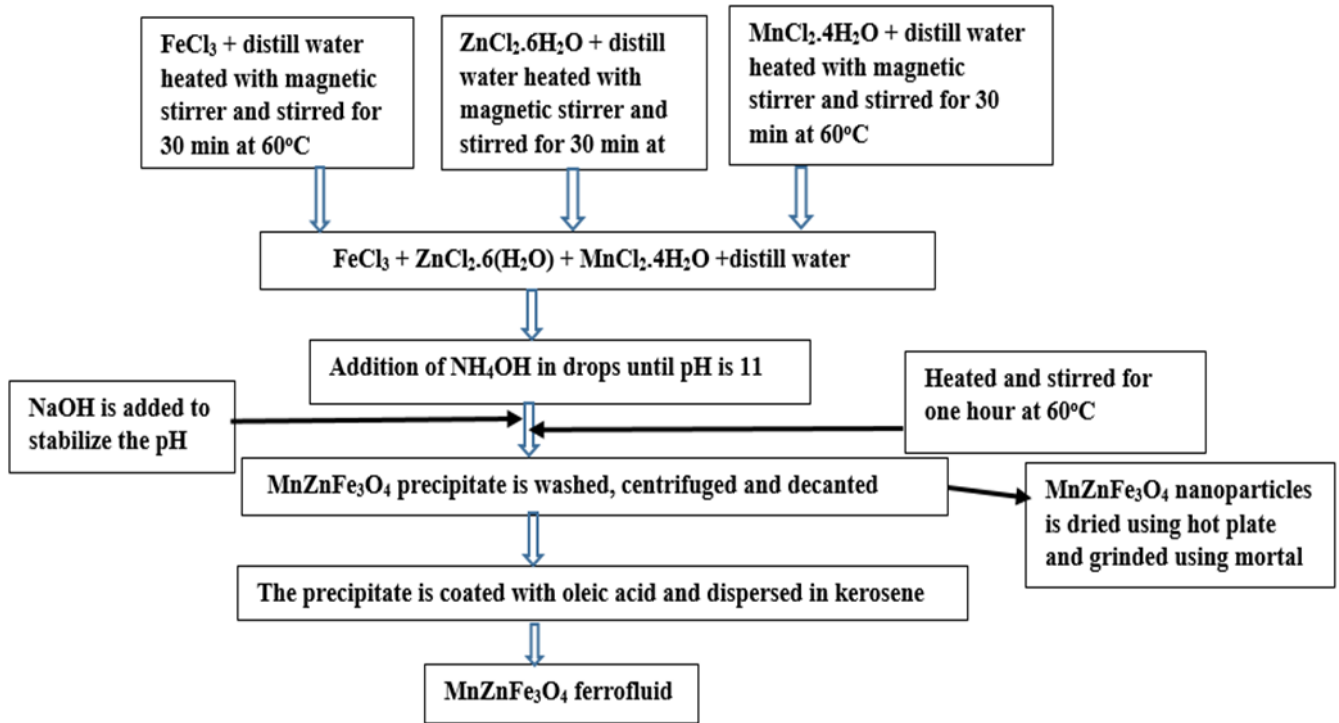
Figure 2. The schematic of the experimental set up of manganese zinc ferrite ferrofluid.
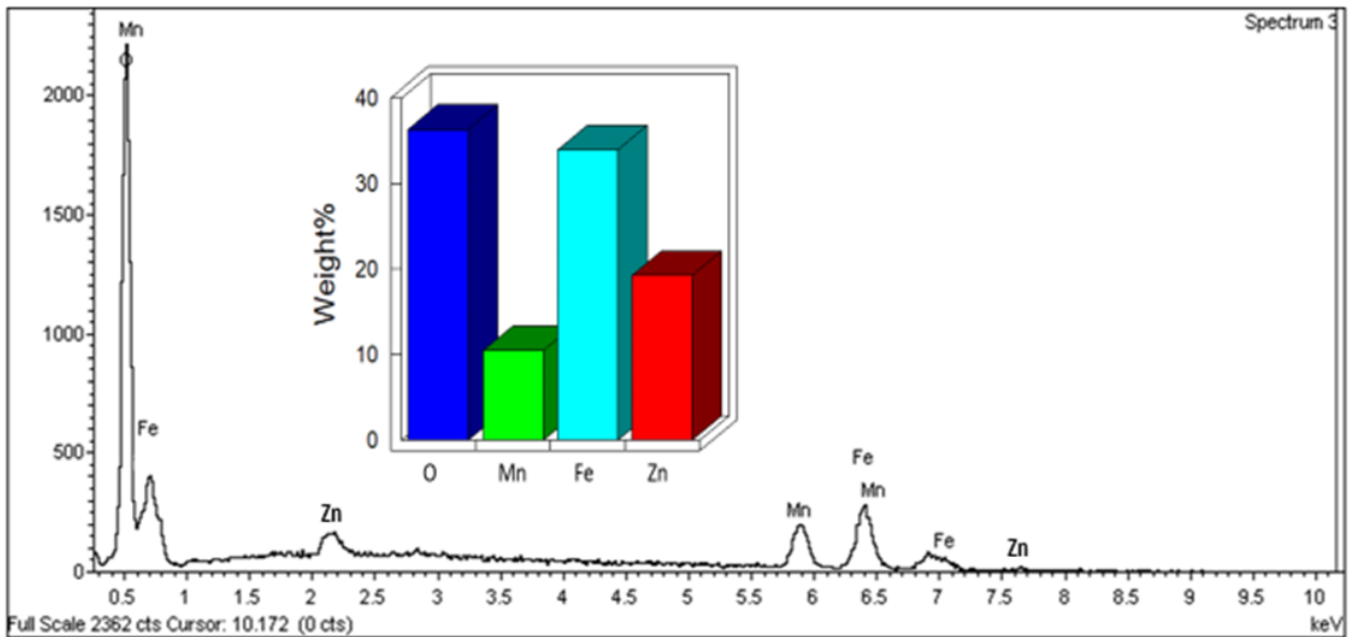

Figure 3. (a) Elemental composition and histogram representation of the quantity of element in weight percentage (b) FTIR spectra of Zn-Mn ferrite magnetic nanoparticles.

of a magnetic field to a fluid particle causes the creation of magnetic chains and magnetically induced structures. Within a magnetic cluster, the particles are magnetically connected to one another. The action of shear stresses on the fluid structure can disassemble these clusters and the magnetic chains. Between 0 and 5 s^{-1}, a region of extremely low shear rate, greater particle interaction results in the creation of rigid/elastic or solid-like structures. This occurred owing to the magnetic chains' resistance to low shear forces and the orderly alignment of the magnetic particles in the direction of the magnetic field rather than the direction of
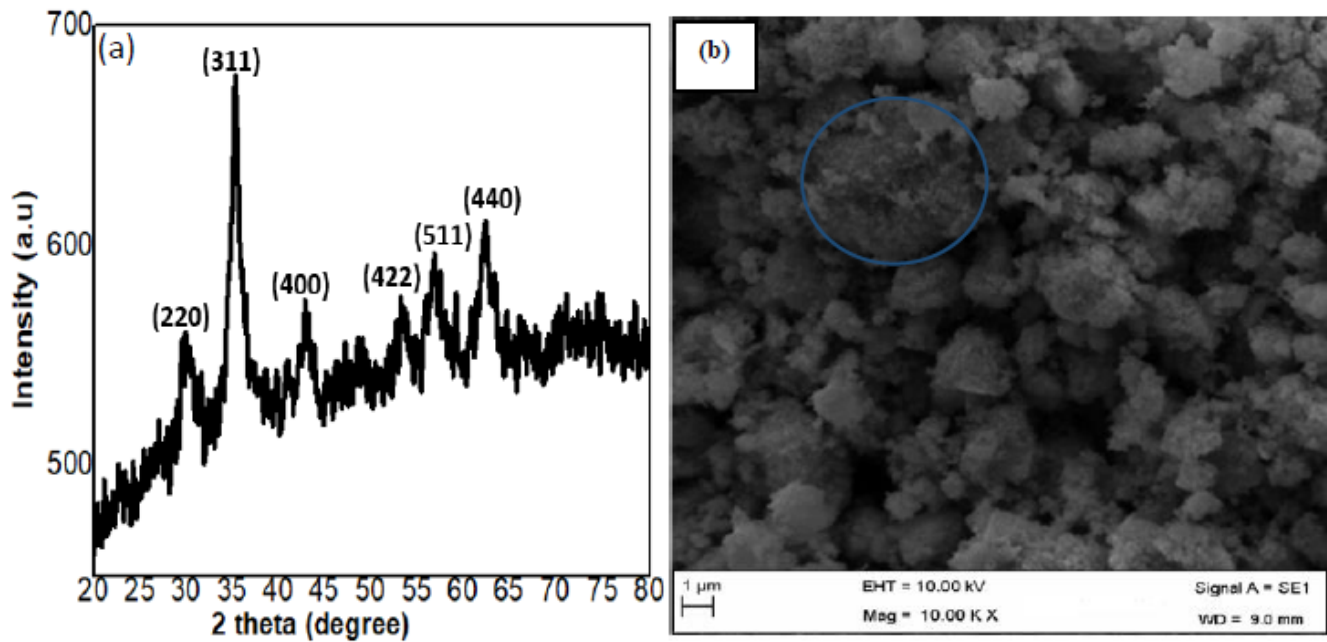
Figure 4. (a) X-ray diffraction, (b) SEM image of Zn-Mn ferrite magnetic nanoparticles.
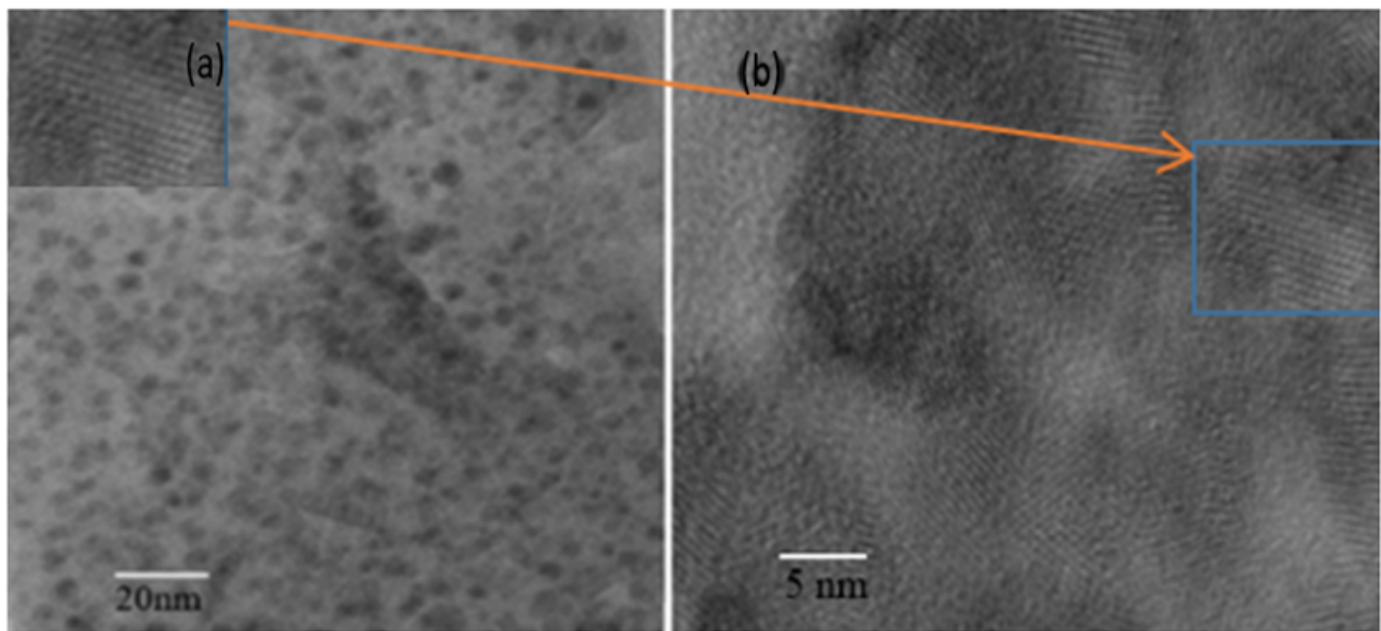

Figure 5. (a) TEM image and (b) HRTEM image of Zn-Mn ferrite magnetic nanoparticles.

the shear, which enhances the formation of highly magnetoviscous fluid that is very resistant to fluid flow. Particles start to move in the shear direction as the shear rate rises, and the fluid structure becomes semi-rigid as the magnetoviscosity falls. This occurred because the applied shear forces modest destruction to the magnetically induced structures and the magnetic clusters. At shear rates between 6 and 10 s^{-1}, a rapid drop in magnetoviscosity is created with increasing shear rate. This occurred because the growing shear force weakens the magnetostatic forces, and

the particle structure is disrupted, which increases the hydrodynamic forces' degree of persistence. A portion of the solid-like structure is destroyed as a result of the hydrodynamic force's increasing resistance to the magnetostatic force, turning a portion of the solid particles into liquid. The fluid structure's rigidity is then thwarted, and as a result of the decrease in magnetoviscosity, it becomes semi-rigid. Within shear rates of 6 to 10 s^{-1}, the fluid demonstrated the creation of non-Newtonian shear thinning effect. The magneto viscous effect decreases at high shear
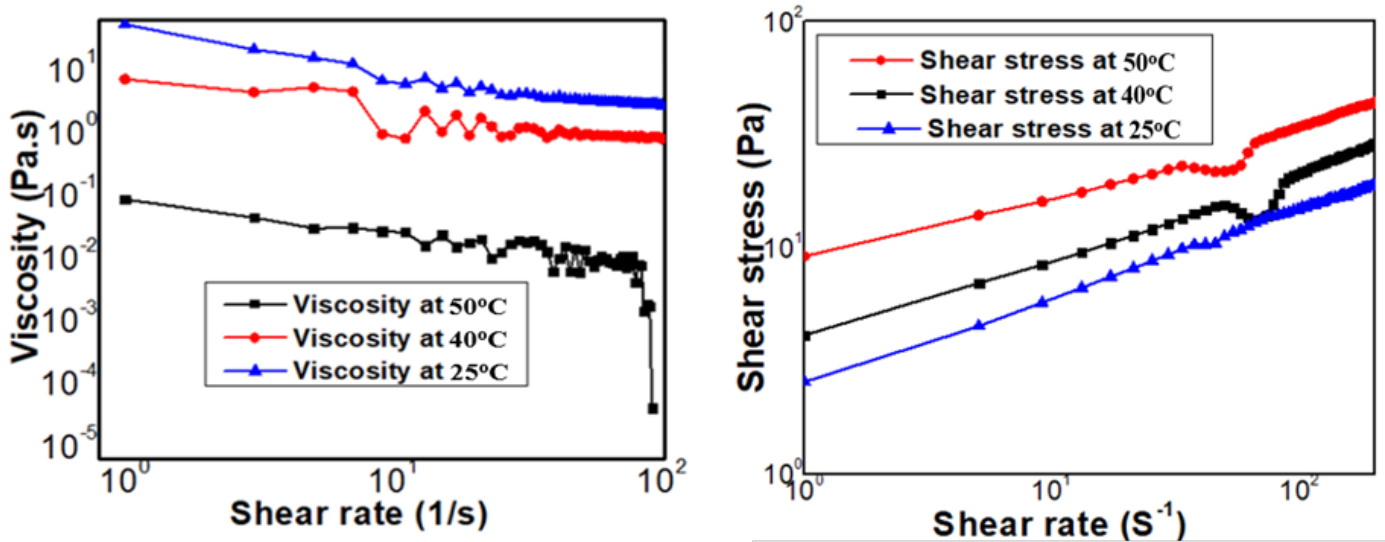
Figure 6. (a) Shear flow of Mn-Zn ferrite ferrofluid (b) shear stress of Mn-Zn ferrite ferrofluid at temperature 25 °C, 40 °C and 50 °C.
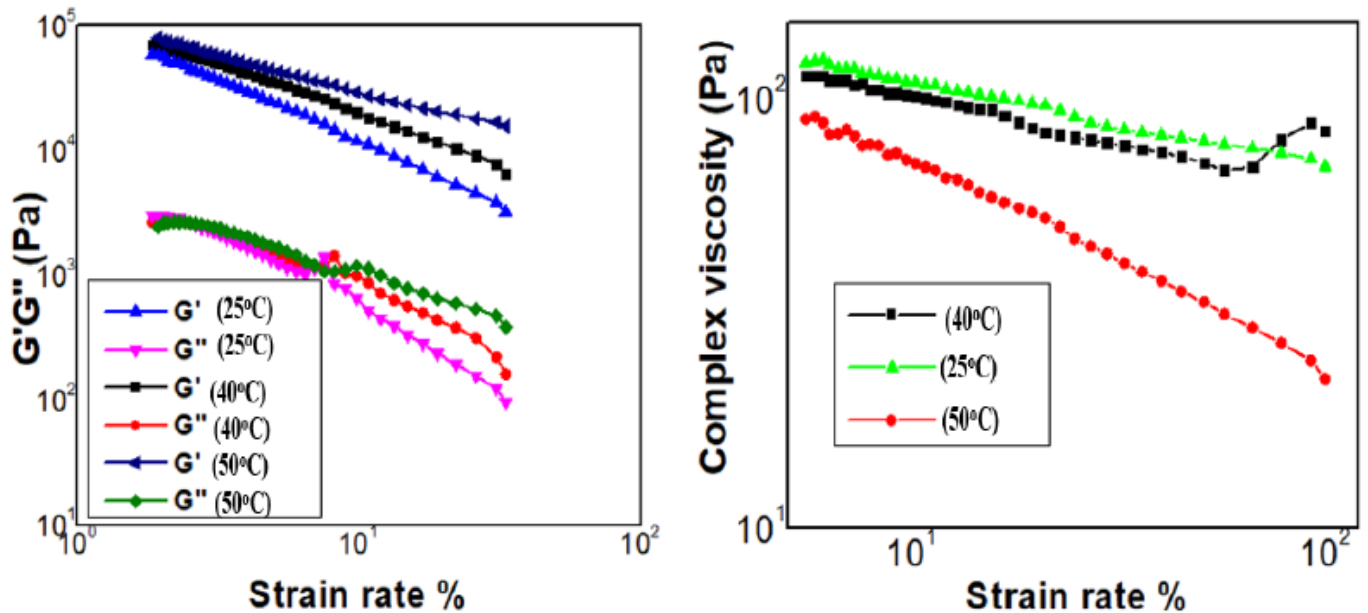

Figure 7. (a) Storage modulus and loss modulus (b) complex viscosity of Mn-Zn ferrite ferrofluid at temperature 25 °C, 40 °C and 50 °C.

rates between 10 and 100 s^{-1} because the magnetic chain cluster is broken to such an extent that the particle clusters are almost completely annihilated. This thinning effect indicates the emergence of low magneto viscous effect as the fluid becomes thinner, softer, and behaves more like Newtonian fluid. Due to the magnetic aggregates' inability to withstand the high shear force, low magnetoviscosity is produced at high shear rates. As a result, the magnetic aggregates are destroyed and the particles separate from the parent aggregates.

High magneto viscous effect is formed when low temperature (25 °C) is applied to the fluid structure. Low temperature causes the formation of low thermal energy, which is less resistant to the binding energy that binds the particles to the aggregates, preventing the breakdown of the magnetic aggregates and making the

fluid rigid due to high magnetoviscosity. When the temperature is raised to 40 °C, a drop in magnetoviscosity develops because the higher temperature partially eliminates the magnetically induced structures. The destruction of the magnetic aggregation results from the binding energy used to link the particles to the aggregates being overwhelmed by the rising thermal energy; the aggregates are thereafter partially destroyed. The transition from rigid magnetic structure to semi-rigid magnetic structure is explained by this effect. Due to the magnetostatic forces' degradation, the hydrodynamic forces were amplified and the particle aggregate was destroyed [23]. As the temperature is raised to 50 °C, the magnetoviscosity dramatically decreases. This happens because the high temperature destroys the majority of the magnetically generated structures. The binding energy that holds the
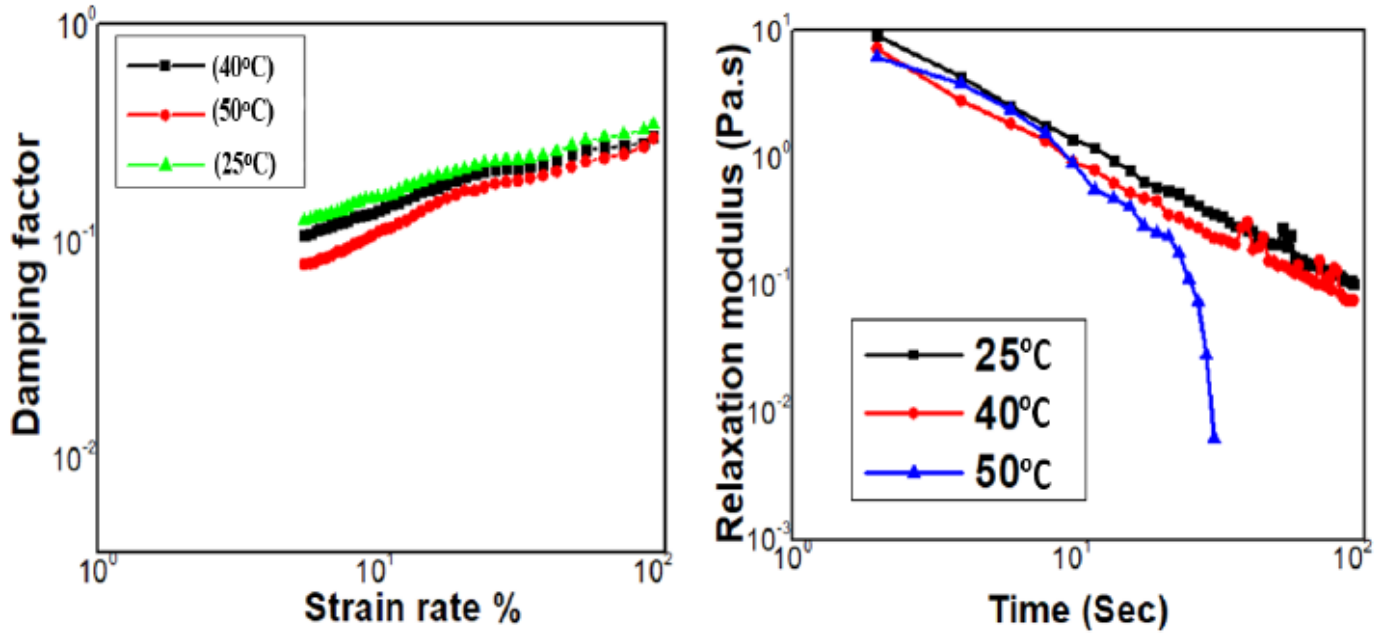
Figure 8. (a) Damping factor and (b) relaxation modulus of Mn-Zn ferrite ferrofluid at temperature 25 °C, 40 °C and 50 °C.
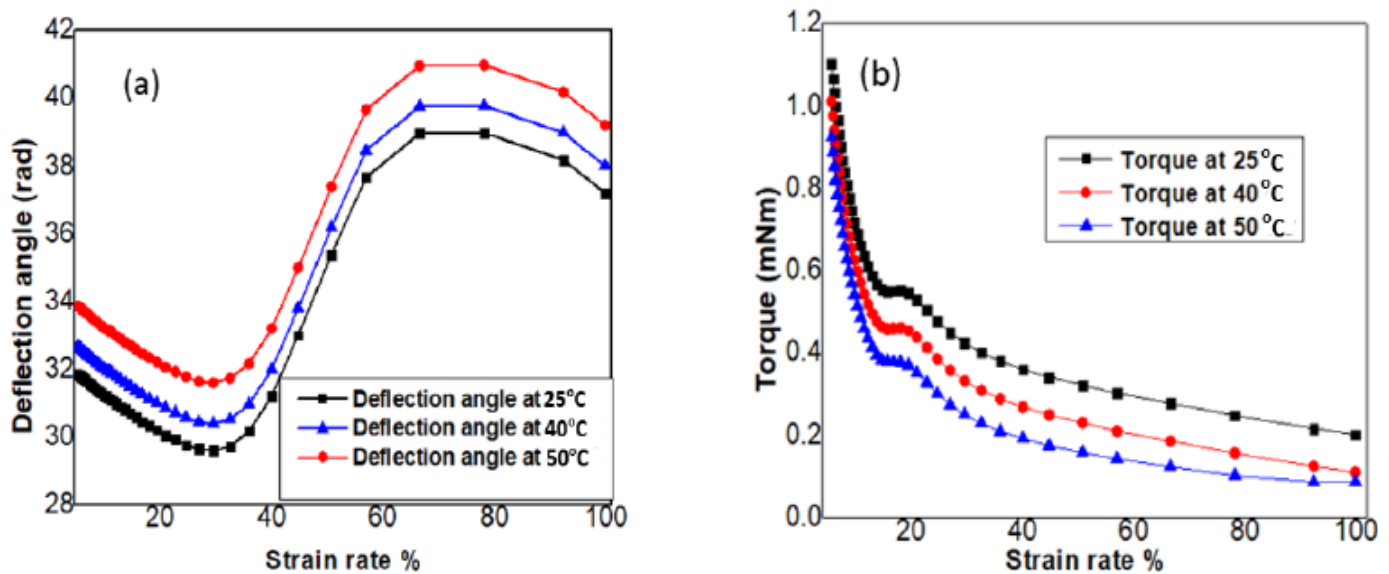

Figure 9. (a) Deflection angle and (b) transmitting torque of Mn-Zn ferrite ferrofluid at different Temperatures.

particles to the magnetic aggregate is eliminated since it is substantially surpassed by the rising thermal energy. As a result, the fluid loses its stiffness and the magnetic structure loses its rigidity. The decrease in magnetoviscosity softens the fluid. Because the cohesive force between the particles is weaker as the temperature rises, the viscosity likewise decreases. The drop in cohesive force resulted from the nanofluid particles' decreased ability to stick together. The intermolecular force of attraction and attractive binding energy that hold the individual particles to the aggregates are forced to weaken and become less resistive when the temperature rises since the average kinetic energy of the fluid

particle likewise increases [24]. The particles were driven to separate from the magnetic aggregates due to the less intermolecular force and binding energy; as a result, the particles are now individual and mobile. As the temperature rises, so does the degree of mobility. Because the attractive binding is weaker, the particle aggregate disintegrates. Maximum viscosity of 50.16 pa.s is achieved at a temperature of 25 °C; this value decreases to 10.35 pa.s and 0.65 pa.s at 40 °C and 50 °C, respectively. This figure is consistent with the highest viscous effects reported by Mishra *et al.* [25], Linke *et al.* [26], and Hosseini *et al.* [27], which were 1.2 pa.s, 2 pa.s, and 9.5 pa.s, respectively. When compar-

ing our results, we can see that larger values of magnetoviscosity are created.

According to Figure 6b, the shear stress rises as the shear rate rises. When a large shear stress is applied, particle aggregate can be destroyed, but when a suitably low shear stress is applied, the aggregate can be protected from damage. The results show that low shear stress cannot destroy the magnetostatic force that holds the particles to the aggregates; as a result, particles stay attached to the aggregates for as long as low shear stress is maintained. Because low shear stress cannot destroy the magnetic structures and the magnetic particles remained attached to the aggregates, high magnetoviscosity at low temperatures is explained. Typically, to generate a stiff magnetic structure and a high magnetoviscosity, a large aggregate of firmly bound particles is required. When the particle aggregate breaks down, the aggregate breaks down because the particles separate from their parent aggregates, and the particles separate from the parent aggregate by the application of a sufficiently high shear stress. Low shear rates produce low shear stresses, and since low stresses cannot dismantle magnetically induced structures, rigid magnetic structures and strong magnetoviscosity is produced. This outcome is consistent with Osial *et al.*'s findings [28], which stated that minimal stress was formed at low shear rates. When the shear rate is between 5 and 10 s^{-1}, the shear stress gradually rises, which causes some fractional destruction of the field-induced structure since the latter is unable to fully withstand the rising shear stress. The fluid becomes thinner because of the disintegration of the structure induced and the fluid's elastic components. A non-Newtonian fluid that is shear thinning forms at shear rates of 5 and 10 s^{-1}. The shear stress is significantly increased at high shear rates greater than 10 s^{-1}. The magnetically induced structures are largely destroyed by a sufficiently strong shear stress, and the links holding the particles together are broken. The magnetic structure is damaged and the magnetostatic force is destroyed by the strong shear stress, which separates the particles from the aggregates later. The particle becomes an individual and moves randomly in the fluid medium after it is separated from the aggregate. When moving quickly, the hydrodynamic force outweighs the magnetostatic force, causing the fluid to become Newtonian and entirely thin [16]. If the yield stress does not exceed the shear stress, a material will not flow. Yield stress is a fluid attribute that a fluid must have in order to flow and that it must reach in order for the fluid to begin flowing. The fluid practically resembles or behaves like elastic material or a stretching spring if yield tension is not attained.

When the temperature of a nanofluid increases, friction between the particle increases as well, weakening the contacts between the particles and creating shear stress. The magnetoviscosity decreases as particle contact decreases. The nanofluid demonstrated a quick rise in shear stress while shear rates are low, and this behavior is effectively captured by Bingham's law:

$$\tau = \tau_B + \eta_P \gamma, \tag{1}$$

where τ is shear stress, τ_B is yield stres, η_P is field dependent viscosity, and γ is shear rate. Results indicate that low shear stress is created at a temperature of 25 °C, but high shear stress is formed at a temperature of 50 °C. The shear force that can damage the fluid's chain structure was assessed using yield stress. As the shear rate rises, the yield stress is exceeded, the particle aggregate fractures, the structure induced by the field is broken and the viscous effect is reduced. The particle aggregates are irreparably destroyed when the shear stress is raised above the critical stress up to a particular degree. The highest stress that the magnetic structure is unable to withstand is known as the yield stress, which is the critical stress. It was discovered that as temperature rises, yield stress decreases.

The findings indicate that low shear stress and high magnetoviscosity are formed at a low temperature of 25 °C. Low temperatures result in the magnetic particles acquiring little thermal energy and thus little shear stress. Because the binding energy that holds the particles to the aggregates is resistive under low stress, the aggregates are now prevented from extinction. As a result, a strong magnetoviscosity and rigid magnetic structure are formed. The thermal state of the fluid system is raised by a temperature increase to 40 °C, which partially eliminates the particle aggregates. Because the binding energy that holds the particles to the aggregates is no longer able to withstand the growing temperature state, the magnetic aggregate is destroyed. Due to this impact, the hard magnetic structure changed into a semi-rigid magnetic structure. When the temperature is raised further, to 50 °C, the magnetoviscosity is dramatically reduced. This happens because the high temperature essentially destroys the particle aggregates. Due to an increase in heat energy, which is very resistant to the binding energy that holds the particles to the aggregates, the magnetic aggregate is destroyed, and the aggregates are subsequently largely destroyed. As a result, the fluid softens due to a decrease in magnetoviscosity, destroying the magnetic structure's stiffness. Because the cohesive force between the particles is weaker as the temperature rises, the viscosity likewise drops. The drop in cohesive force resulted from the nanofluid particles' decreased ability to stick together. The intermolecular force of attraction and attractive binding energy that hold the individual particles to the aggregates are forced to weaken and become less resistive when the temperature rises since the average kinetic energy of the fluid particle likewise increases [23]. The particles were driven to separate from the magnetic aggregates due to the weaker intermolecular force and binding energy.

3.3. STORAGE MODULUS (G'), LOSS MODULUS (G'') AND COMPLEX VISCOSITY OF MN-ZN FERRITE FERROFLUID

The viscoelastic characteristics of Mn-Zn ferrite ferrofluid were investigated using oscillatory sweep test. The ferrofluid's magnetoviscoelastic system is studied in relation to temperature. As seen in Figure 7a, the storage modulus (G') is obviously greater than the loss modulus (G'') at all strain rates. According to studies, the storage modulus (G') of the viscoelastic system determines both the absolute energy stored and the elastic behavior. Additionally, the size of the loss modulus (G'') determines the viscous property and the rate at which energy is lost from the viscoelastic system. Since the elastic modulus dominates the loss modulus at low strain rates, a dominating elastic structure with a sizable solid-like structure is likely to arise. As a result of the system being dominated by magnetostatic forces, this indicates the creation of stronger linkages among the magnetic nanoparticles [16]. Although the fluid's solid-like structure still outweighs

its liquid-like structure despite an increase in strain rate, the connection between the particles there is slightly weaker. The elastic structure is now maintained and has won over the viscous structure since a cross over point cannot be established across the curves indicated by the storage and loss modulus. Since there isn't a transition from a solid-like to a liquid-like state, G' and G" don't cross over at all. Given that G' > G", the fluid has a high energy storage capacity. The findings of this study are consistent with those of Mahesh *et al.*, who do not mention any phase transitions [20]. The fluid exhibits less improved viscoelastic behavior at a temperature of 25 °C, whereas enhanced viscoelastic structure forms at a temperature of 50 °C. There is no structural rearrangement at any temperature since the loss modulus is linear and extremely close to zero. In contrast to what Balaji *et al.* reported, enhanced viscoelasticity is created with a maximum elastic value of the order 10^5, which is nearly ten times higher. Balaji *et al.* showed a rise in storage and loss modulus with increasing rotational frequency [29]. G' is significantly bigger than G", which indicates the production of an elastic dominant structure and a solid-like nanofluid with the formation of a phase transition at high strain amplitude, Yongbo *et al.* got a result that is accurately in accordance with the current experimental finding [30]. The dependence of elastic modulus on strain was demonstrated by Mitsumata and Okazaki, and the modulus increases with strain [31], this fact has been re-established in this present research work. The storage modulus decreases as the strain rate increases; however, Wagner *et al.* observed that the storage modulus increases as the angular frequency increases [32].

At various temperatures, we performed oscillatory frequency sweep tests on Mn-Zn ferrite ferrofluid. Figure 7b shows that complex magnetoviscosity decreases as strain rate increases. Because the imposed low strain did not cause the magnetically induced structure to deform, stronger linkages were established by the particles during their contact in the low strain rate area, leading to the production of high complex magnetoviscosity. The findings demonstrate that a non-Newtonian fluid forms under mild strain applications. The interaction between the interacting particles weakens gradually for strain rates between 5% and 20%, which results in the development of diminishing complex magnetoviscosity. The fluid thins as the particle aggregate disintegrates, partially separating the particles from the aggregate. The complex magneto viscous action of the fluid is lessened at high strain rates between 20% and 100% because the chain structure is sufficiently deformed by the high strain that the particle aggregates are all but completely obliterated. This thinning effect is a feature of low complex magneto viscous effect and liquid-like fluid. The fluid thins out and conducts itself like Newtonian fluid. Increased strain rate causes a complex viscous effect to diminish. Because the field-induced structure fractures at high strain rates and the particles separate from the aggregates, and the complex viscosity decreases. The aggregate is completely damaged with further strain rate increase, which softened the fluid by creating a low viscosity effect [33, 34]. Complex magnetoviscosity rises as temperature falls [35]. The chain structure and particle aggregate are unable to withstand the tremendous thermal energy that the fluid components exhibit at high temperatures; as a result, the chains disintegrate and the particles separate from the aggregate into units. Since the particles have separated from the aggregates,

they are now mobile, and as the temperature rises from 25 °C to 50 °C, the mobility of the particles increases. Additionally, as the temperature rises, the cohesion between the particles weakens while their average kinetic energy rises. These two effects support the destruction of the attractive binding energy and the separation of the particles from the aggregates.

3.4. DAMPING FACTOR AND RELAXATION MODULUS OF MN-ZN FERRITE FERROFLUID

Due to its appropriate particle stability in the carrier medium, ferrofluid is helpful for effective dampening applications and efficient heat control systems, according to recent research. The creation of effective damping applications and heat control systems is aided by several additional ferrofluid characteristics, such as longetivity and zero leakages. Ferrofluid responds to magnetic fields, but non-magnetic fluids like parafin, water, kerosene, etc. do not, making it suitable for effective heat management systems. Prior to the invention of ferrofluid, non-magnetic fluids were created for use as heat controls, heat exchangers, and dampers. However, because these fluids have low thermal conductivity, their effectiveness as controls and dampers is diminished. A magnetic fluid, such as ferrofluid, is designed to replace the non-magnetic fluids in order to achieve an efficient system. Due to ferrofluid's high thermal conductivity, it has been successfully applied in a variety of applications as a damper and heat controller. Ferrofluiod (FF) is a better damper due to its flexibility, dependability [36], and small nanoscale particle sizes. The ineffectiveness of non-magnetic fluids can be attributed to the fluid particles' instability in the base medium and their changeable rheological characteristics over time [37]. In a viscoelastic system, the damping factor and energy loss determine the damper's strength. Based on the value of the damping factor, damping is divided into three categories: overdamping, critical damping, and underdamping [38]. Our findings showed that an underdamped viscoelastic system had formed because, as shown in Figure 8a, the damping factor of the system is less than one. This happened as a result of the system being dominated by elastic particles, and the effect is attributed to the system dissipating a little amount of energy. Due to the production of high storage moduli and low loss moduli, there was limited energy dissipation. Because Mn-Zn ferrite ferrofluid is underdamped, it cannot be employed in systems that require effective heat management or damping and has a low energy dissipation. Low damping indicates that there is sufficient energy stored in the system and that there is little energy lost when the rate of strain is low. Due to its extremely low energy loss, the system does not display any active damping states at temperature 50 °C, where the damping factor value is almost zero. A rheological system is created with a maximum damping ratio of 0.25, which is higher than the 0.16 value reported by Rao *et al.* [39]. These numbers are not high enough to support the usage of Mn-Zn ferrofluid as a heat control or damper.

The viscoelastic system is kept from being perturbed by the relaxation modulus, a rheological parameter that controls the stress applied to a sample and helps it return to equilibrium after being sheared [40, 41]. When temperature of 25 °C is applied, non-linear relaxation modulus and a non-steady state flow are established within interval of 30 seconds, as shown in Figure 8b. At a

time interval after 30 s, a linear relaxation modulus and a steady state fluid outflow were produced. The system utilizes less time to launch a steady state fluid outflow at temperature 50 °C when compare with temperature 25 °C. This shows that stabilized fluid flow is promptly launched at high temperature but takes longer time to be launched at low temperature. When temperature 40 °C is supplied, a steady state flow forms within 10 s; however, the system takes longer to relax at 40 °C than it does at 25 °C. At a temperature of 50 °C, a negative relaxation forms after 2 seconds, and after another 2 seconds, a linear relaxation modulus that denotes the establishment of a stable fluid outflow forms. The results demonstrate that temperature affects the emergence of a stable condition for fluid outflow. All applied temperatures of 25 °C, 40 °C, and 50 °C during 30 s, 10 s, and 2 s, respectively, result in stable state fluid flow.

3.5. DEFLECTION ANGLE AND TRANSMITTING TORQUE OF MN-ZN FERRITE FERROFLUID

Experimental research is done to determine how ferrofluid deflection affects the rheology of Mn-Zn ferrofluid. According to studies, fluid deflection is a crucial factor in the hardening and softening of fluid, and the shear flow is influenced by the size of the deflection angle. The results demonstrate that when compared to huge volumes of fluid deflected at high strain rates, the volume of fluid deflected at low strain rates is small. Previous studies revealed that the physico-mechanical system of the ferrofluid changes when a significant portion of it is deflected. Large volumes of rigid/elastic fluid deflect, losing their stiffness and becoming semi-rigid. Figure 9a illustrates the creation of a tiny deflection angle under low strain, which prevents the ferrofluid from deflecting in large volumes. One of the reasons the ferrofluid is substantially elastic at a location where low strain rate is prevalent is because low volume of the ferrofluid is deflected, maintaining the fluid's rheological features such as rigidity. This demonstrates how the behavior of ferrofluids depends on the fluid deflection angle and volume. The deflection angle increases with increasing strain rate. Large deflection angles support the deflection of large volumes of ferrofluid in areas where high strain rates are predominant. One of the reasons the ferrofluid is primarily viscous and less rigid at high strain rate region is because a huge volume of the fluid is deflected, which destroys the fluid's rheological qualities like rigidity. Increased strain rate causes the deflection angle to broaden, which causes a significant amount of ferrofluid to be deflected. This happened as a result of the fluid's ability to deflect being unrestricted by the wide deflection angle. When there is minimal strain rate, low deflection angles arise, preventing the fluid from deflecting. Large volumes of fluid are prevented from deflecting by the decreased deflection angle at low strain rates, whereas the deflection angle widens at high strain rates. One of the reasons the ferrofluid is primarily viscous and less rigid at high strain rate region is because a huge volume of the fluid is deflected, which destroys the fluid's rheological qualities like rigidity. Increased strain rate causes the deflection angle to broaden, which causes a significant amount of ferrofluid to be deflected. This happened as a result of the fluid's ability to deflect being unrestricted by the wide deflection angle. When there is minimal strain rate, low deflection angles arise, preventing the fluid from deflecting. Large volumes

of fluid are prevented from deflecting by the decreased deflection angle at low strain rates, whereas the deflection angle widens at high strain rates.

It can be seen that the degree of ferrofluid deflection at the application of high temperature is large compared with degree of ferrofluid deflection when low temperature is applied. At a low temperature, small deflection angle is formed as shown in Figure 9a, the small deflection angle restricts the deflection of large volume of ferrofluid, owing to narrowing of the deflection angle when a low temperature is applied. The results demonstrate that as the temperature rises, the deflection angle widens and increases, leading to the deflection of a significant portion of a ferrofluid sample. Enormous volume of ferrofluid can be deflected owing to the broadening of the deflection angle. Due to the creation of a modest deflection angle at a low temperature, the little volume of fluid deflected. However, when high temperatures are applied, a significant volume of fluid is deflected because a high deflection angle is created. The viscosity of the ferrofluid and internal frictional force of the molecular chains, which rearrange the fluid characteristics, are thought to be the causes of the difference in deflection angle.

A reduction in transmitting torque at high temperatures is shown in Figure 9b. It is evident that using a high temperature causes the system's thermal energy and thermal expansion to increase, and that this expansion reduces the nanofluid's lifetime and durability [44]. Due to a reduction in torque as the temperature rises, the resistance decreases. Since high viscous fluid molecules are compact and densely packed and exhibit significant levels of internal friction, driving a high viscous fluid typically necessitates a large amount of torque. As a result of the ferrofluid's molecules not being crushed and tightly packed, the results demonstrate that low viscous fluid requires little torque to move the fluid's particles. At high temperatures, the fluid expands due to the thermal effect, which causes a reduction in transmitted torque. The researcher discovered attenuation and a decrease in torque [45], which impeded the endurance of the ferrofluid sample at high temperature. The conclusion is consistent with the findings by Wiehe *et al.* This was confirmed by Wang *et al.*, who demonstrated that the increased temperature decreased the viscous torque [46]. Francesco *et al.* also found a decrease in transmitted torque as the temperature is increased [47]. From 25 °C to 50 °C, torque decreases as temperature rises. High temperatures produce little torque, whereas low temperatures produce high torque. A certain amount of energy is consequently needed to fight the Brownian motion of the nanometer-sized particles and construct a chain-like structure that exhibits huge particle aggregates since Brownian motion has an adverse effect on the stability of the particle. As a result, the magnetic structure's stability is reduced, which causes transmitted torque to decrease as temperature rises.

4. CONCLUSION

It was investigated how temperature affected the rheology of Mn-Zn ferrite ferrofluid. The presence of big particle aggregates causes the fluid to exhibit significant magnetoviscosity at low temperatures. Due to the presence of both a viscous and an elastic structure, the ferrofluid of Mn-Zn ferrite is viscoelastic. The creation of a large elastic structure and a very little viscous compo-

nent is implied by the storage modulus being significantly bigger than the loss modulus. At 25 °C, large complex viscosity is created, and as temperature rises, shear stress decreases. Low shear rates result in low shear stress. As the temperature rises, there is a loss of transmitting torque. When ferrofluid is flowing freely, part of it can deflect, which has a big impact on how fluids harden and soften. Due to the system's damping factor being less than one, we documented the emergence of an underdamped system. The application of temperatures of 25°C, 40 °C, and 50 °C for 30 seconds, 10 seconds, and 2 seconds, respectively, results in the creation of steady state flow, which is temperature-dependent.

References

[1] N. Jahan, S. Pathak, K. Jain & R. P. Pant, "Enhancement in viscoelastic properties of flake-shaped iron based magnetorheological fluid using ferrofluid", Colloids Surface A: Physico chem. Eng. Aspects. **529** (2017) 88. https://doi.org/10.1016/j.colsurfa.2017.05.057.

[2] V. Kumar, A. Rana, M. S. Yadav & R. P. Pant, "Size-induced effect on nanocrystalline $CoFe_2O_4$", Journal of Magnetism and Magnetic Material**320** (2008) 1729. https://doi.org/10.1016/j.jmmm.2008.01.021.

[3] N. Jahan, G. A Basheed, K. Jain, S. Pathak & R. P. Pant, "Dipolar interaction and magneto-viscoelasticity in nanomagnetic fluid", Journal of Nanoscience and Nanotechnology 18 (2018) 2746. https://doi.org/10.1166/jnn.2018.14532.

[4] P. Sharma, V. V. Alekhya, S. Pathak, K. Jain, P. Tomar, G. A. Basheed, K. K. Maurya & R. P. Pant, "A novel experimental approach for direct observation of magnetic field induced structuration in ferrofluid", Journal of Magnetism and Magnetic Materials **534** (2021) 168024. https://doi.org/10.1016/j.jmmm.2021.168024.

[5] K. Jain, S. Pathak & R. P. Pant, "Enhanced magnetic properties in ordered oriented ferro fibres", RSC Advances 6 (2016) 70943. https://doi.org/10.1039/C6RA12650B.

[6] P. Shima, P. John and R. Baldev, "Magnetically controllable nanofluid with tunable thermal conductivity and viscosity", Applied Physics Letter **95** (2009) 133112. https://doi.org/10.1063/1.3238551.

[7] S. E. Premalatha, R. Chokkalingam & M. Mahendran, "Magneto Mechanical Properties of Iron Based MR Fluids, American Journal of Polymer Science", **2** (2012) 50. https://doi.org/10.5923/j.ajps.20120204.01.

[8] S. Singamaneni, V. N. Bliznyuk, C. Binek & E. Y. Tsymbal, "Magnetic nanoparticles: recent advances in synthesis, self-assembly and applications", Journal of Material and Chemistry 21 (2011) 16819. https://doi.org/10.1039/c1jm11845e.

[9] X. K. Chen & K. Q. Chen, "Thermal Properties of carbon nanomaterials", Journal of Physics Condensed Matter 32 (2020) 153002. https://doi.org/10.1088/1361-648X/ab5e57.

[10] P. Shima, P. John & R. Baldev, "Magnetically controllable nanofluid with tunable thermal conductivity and viscosity", Applied Physics Letter **95** (2009) 133112. https://doi.org/10.1063/1.3238551.

[11] X. K. Chen, X. Y. Hu, P. Jia, Z. X. Xie & J. Liu, "Tunable anisotropic thermal transport in porous carbon foams: The role of phonon coupling", International Journal Mech Science **206** (2021) 106576. https://doi.org/10.1016/j.ijmecsci.2021.106576.

[12] L. A. Powell, W. Hu and N. M. Wereley, "Magnetorheological fluid composites synthesized for helicopter landing gear applications", Journal of Intelligent Material System Structure **24** (2013) 1043. https://doi.org/10.1177/1045389X13476153.

[13] G. Paul, P. K. Das and I. Manna, "Synthesis, characterization and studies on magneto-viscous properties of magnetite dispersed water based nanofluids", Journal of Magnetism and Magnetic Material **404** (2021) 29. https://doi.org/10.1016/j.jmmm.2015.11.085.

[14] T. Liu, X. Gong, Y. Xu and S. Xuan, "Magneto-induced stress enhancing effect in a colloidal suspension of paramagnetic and superparamagnetic particles dispersed in a ferrofluid medium", Soft Matter **10** (2014) 813. https://doi.org/10.1039/c3sm52865k.

[15] K. Shahrivar, A. L. Ortiz and J. A de Vicente, "Comparative study of the tribological performance of ferrofluids and magnetorheological fluids within steel–steel point contacts", Tribology International **78** (2014) 25. https://doi.org/10.1016/j.triboint.2014.05.008.

[16] K. Shah, J. S. Oh, S. B. Choi & R. Upadhyay, "Plate-like iron particles based bidisperse magnetorheological fluid", Journal of Applied Physics

[17] H. Anwar, A. Maqsood & I. H. Gul, "Effect of synthesis on structural and magnetic properties of cobalt doped Mn-Zn nano ferrites", Journal of alloys and compounds **626** (2015) 410. https://doi.org/10.1016/j.jallcom.2014.11.177.

[18] A. A Ibiyemi, O. Akinrinola & G. T. Yusuf, "Photoelectric and optoelectronic effects of hard ferromagnetic manganese cobalt (Mn-Co) ferrite nanoparticles for high frequency device application", Applied physics A; material science and processing **128** (2022) 792. https://doi.org/10.1007/s00339-022-05926-x.

[19] V. Šepelah, I. Bergmann, A. Feldhoff, P. Heitjans, K. Frank, M. Dirk, J. Fred, S. J. Campbell and D. Klaus, "Nanocrystalline nickel ferrite, $NiFe_2O_4$: mechanosynthesis, nonequilibrium cation distribution, canted spin arrangement, and magnetic behavior", The Journal of Physical Chemistry **C 111** (2019) 5026. https://doi.org/10.1007/s10751-006-9251-3.

[20] M. Ajmal & A. Maqsood, "AC conductivity, density related, and magnetic properties of $Ni_{1-x}Zn_xFe_2O_4$ ferrites with the variation of zinc concentration", Material Letters **62** (2008) 2077-2080. https://doi.org/10.1016/j.matlet.2007.11.019.

[21] A. Mishra, S. Pathak, P. Kumar, A. Singh, K. Jain, R. Chaturvedi, D. Singh, G. A. Basheed & R. P. Pant, "Measurement of Static and Dynamic Magneto-Viscoelasticity in Facile Varying pH Synthesized $CoFe_2O_4$-Based Magnetic Fluid", IEEE Transactions on Magnetics **55** (2021) 4601107. https://doi.org/10.1109/TMAG.2019.2936802.

[22] B. K. Kumbhar, S. R. Patil and S. M. Sawan, "Synthesis and characterization of magnetorheological (MR) fluids for MR brake application", Engineering Science and Technology, an International Journal **18** (2021) 432. https://doi.org/10.1016/J.JESTCH.2015.03.002.

[23] A. A Ibiyemi, G. T. Yusuf, O. Olubosede, A. Olusola and H. A Akande, " Photoelectric and magnetic properties of chemically synthesized Cd–Ni Ferrite nanomagnetic particles", Physica Scripta **97** (2022) 025804. https://doi.org/10.1088/1402-4896/ac4a95.

[24] A. A. Ibiyemi, G. T. Yusuf and A. Olusola, "Influence of temperature and magnetic field on rheological behavior of ultra-sonicated and oleic acid coated cobalt ferrite ferrofluid", Physica scripta **96** (2021) 125842. https://doi.org/10.1088/1402-4896/ac2ecb.

[25] D. Y. Borin, V. V. Korolev, A. G. Ramazanova, S. Odenbach, O. V. Balmasova, V. I. Yashkova & D. V. Korolev, "Magneto viscous effect in ferrofluids with different dispersion media", Journal of Magnetism and Magnetic Material **416** (2016) 110. https://doi.org/10.1016/J.JMMM.2016.05.024.

[26] J. M. Linke & S. Odenbach, "Anisotropy of the magneto viscous effect in a ferrofluid with weakly interacting magnetite nanoparticles", Journal of Physics: Condensed Matter **27** (2015) 176001. https://doi.org/10.1088/0953-8984/27/17/176001.

[27] H. Masoud, L. Vafajoo, E. Ghasemi & B. H. Salman, "Experimental investigation the effect of nanoparticle concentrationon the rheological behavior of paraffin-based nickel ferrofluid", International Journal of Heat Mass Transfer **93** (2016) 228. https://doi.org/10.1016/j.ijheatmasstransfer.2015.09.082.

[28] M. Osial, M. Nowicki, E. Klejman & L. Fras, "Investigation of well-dispersed magnetorheological oil-based suspension with superparamagnetic nanoparticles using modified split Hopkinson pressure bar", Rheological Acta **61** (2022) 111. https://doi.org/10.1007/s00397-021-01318-9.

[29] V. S. Balaji, V. Y. Victor & C. B. Anna, "Dynamic behavior of dual cross-linked nanoparticle networks under oscillatory shear", New Journal of Physics **16** (2014) 075009. https://doi.org/10.1088/1367-2630/16/7/075009.

[30] Y. Yongbo, L. Lin, C. Guang & L. Weihua. Magnetorheological properties of aqueous ferrofluid. Journal of the Society of Rheology **24** (2005) 25. https://doi.org/10.1678/rheology.34.25.

[31] T. Mitsumaka & T. Okazaki, "Magnetization-induced reduction in dynamic modulus of polyurethane elastomers loaded with ferrite", Japanese Journal of Applied Physics **46** (2007) 4220. https://doi.org/10.1143/JJAP.46.4220.

[32] M. H. Wagner, E. Narimissa & T. Shahid, "Elongational viscosity and brittle fracture of bidispersed blends of a high and several low molar mass polystyrenes", Rheological Acta **60** (2021) 803. https://doi.org/10.1007/s00397-021-011304-1.

[33] Y. Li, P. Han, D. Li, S. Chen and Y. Wang, "Typical dampers and energy harvesters based on characteristics of ferrofluids", Friction **11** (2023) 165. https://doi.org/10.1007/s40544-022-0616-7.

[34] D. Borin, R. Müller & S. Odenbach, "Magnetoviscosity of a Magnetic Fluid Based on Barium Hexaferrite Nanoplates", Materials **14** (2021) 1870.

114 (2013) 213904. https://doi.org/10.1063/1.4837660.

https://doi.org/10.3390/ma14081870.

[35] M. J. Pastoriza-Gallego, M. Pérez-Rodríguez, C. Gracia-Fernández & M. M. Piñeiro, ''Study of viscoelastic properties of magnetic nanofluids: An insight into their internal structure'', Soft Matter **9** (2013) 11690. https://doi.org/10.1039/c3sm51952j.

[36] A. A. Ibiyemi & R. P. Pant, "A trivalent ferrite ferrofluid compound's rheological response to angular frequency, magnetic induction and shear induction of chain clusters'', Physica Scripta (2023) https://doi.org/10.1088/1402-4896/ad094c.

[37] J. J. Vadasz, G. Saneshan and V. Peter, ''Heat transfer enhancement in nanofluids suspensions: possible mechanism and explanations'', International Journal of Heat and Mass Transfer **48** (2005) 2673. https://doi.org/10.1016/j.ijheatmasstransfer.2005.01.023.

[38] A. A. Ibiyemi & G. T. Yusuf, ''Rheological Investigation of Strain Rate and Magnetic Field on the Magnetorheology of Zinc Ferrite Ferrofluid'', Applied Physics A **128** (2022) 591. https://doi.org/10.1088/1402-4896/ac2ecb.

[39] M. D. Rao, P. S. Goyal, B. Panda & R. I. K. Moorthy, ''Ferrofluids for Active Shock Absorbers'', Materials Science and Engineering **360** (2018) 012002 https://doi.org/10.1088/1757-899X/360/1/012002.

[40] C. Upadhyay, H. C. Verma and S. Anand, ''Cation distribution in nanosized Ni–Zn ferrites'', Journal of Applied Physics **95** (2004) 5746. https://doi.org/10.1063/1.1699501.

[41] J. P. Segovia-Gutierrez, J. de Vicente, R. Hidalgo-Alvarez & A. M. Puertas, ''Brownian dynamics simulations in magnetorheology and comparison with experiments'', Soft Matter **9** (2013) 6970. https://doi.org/10.1039/C3SM00137G.

[42] C. Hou, H. Yu, Q. Zhang, Y. Li and H. Wang, ''Preparation and magnetic property analysis of monodisperse Co–Zn ferrite nanospheres'', Journal of Alloys Compound **491** (2010) 431. https://doi.org/10.1016/j.jallcom.2009.10.217.

[43] R. Topkaya, A. Baykal and A. Demir, ''Yafet–Kittel-type magnetic order in Zn-substituted cobalt ferrite nanoparticles with uniaxial anisotropy'', Journal of nanoparticle research **15** (2013) 1359. https://doi.org/10.1007/s11051-012-1359-6.

[44] J. A. Ruiz-López, Z. W. Wang, R. Hidalgo-Alvarez & J. de Vicente, ''Simulations of model magnetorheological fluids in squeeze flow mode'', Journal of Rheology **61** (2017) 871. https://doi.org/10.1122/1.4990641.

[45] A. Wiehe, C. Kieburg & J. Maas, ''Temperature induced effects on the durability of MR fluids'', Journal of Physics: Conference Series **412** (2013) 012017. https://doi.org/10.1088/1742-6596/412/1/012017.

[46] D. Wang, B. Zi, Y. S. Zeng & F. W. Xie, ''An investigation of thermal characteristics of a liquid-cooled magnetorheological fluid-based clutch'', Smart Material Structure **24** (2015) 055020. https://doi.org/10.1007/s13367-021-0024-y.

[47] B. Francesco, F. Paola & F. Francesco, ''Temperature effect on the torque characteristic of a magnetorheological clutch", Mechanics of advanced materials and structures **22** (2015) 150. https://doi.org/10.1080/15376494.2014.910581